arXiv:1605.07034v1 [quant-ph] 23 May 2016

Entanglement in the Born-Oppenheimer Approximation

Artur F. Izmaylov*
Department of Physical and Environmental Sciences, University of Toronto Scarborough, Toronto, Ontario, M1C 1A4, Canada; and Chemical Physics Theory Group, Department of Chemistry, University of Toronto, Toronto, Ontario, M5S 3H6, Canada

Ignacio Franco†
Department of Chemistry and The Center for Coherence and Quantum Optics, University of Rochester, Rochester, New York 14627, USA

(Dated: March 8, 2022)

The role of electron-nuclear entanglement on the validity of the Born-Oppenheimer (BO) approximation is investigated. While nonadiabatic couplings generally lead to entanglement and to a failure of the BO approximation, surprisingly the degree of electron-nuclear entanglement is found to be uncorrelated with the degree of validity of the BO approximation. This is because while the degree of entanglement of BO states is determined by their deviation from the corresponding states in the crude BO approximation, the accuracy of the BO approximation is dictated, instead, by the deviation of the BO states from the exact electron-nuclear states. In fact, in the context of a minimal avoided crossing model, extreme cases are identified where an adequate BO state is seen to be maximally entangled, and where the BO approximation fails but the associated BO state remains approximately unentangled. Further, the BO states are found to not preserve the entanglement properties of the exact electron-nuclear eigenstates, and to be completely unentangled only in the limit in which the BO approximation becomes exact.

I. INTRODUCTION

The Born-Oppenheimer (BO) approximation forms the basis of our interpretation of chemical phenomena. As a consequence, considerable effort has been devoted to understand its scope, and to develop methods that allow us to think and model matter beyond its limits [1–8]. Surprisingly, however, an unexplored aspect of the BO approximation is its connection with entanglement [9, 10], a basic quantum-mechanical correlation that is the essential resource for quantum information [11]. In addition to its interest at a fundamental level, understanding the role of entanglement in the BO picture is central in interpreting coherence phenomena in matter and in the development of methods to follow correlated electron-nuclear dynamics. Specifically, to be able to capture all relevant quantum correlations, approximate semiclassical or quantum descriptions of the electron-nuclear evolution of molecules [1, 2, 4, 12, 13] should preserve the entanglement character of the electron-nuclear states. Further, the understanding of coherence phenomena in molecules [14–21], such as coherent spectroscopies, photoexcited dynamics and electron transfer events, requires a detailed understanding of the molecular events that lead to electronic decoherence through entanglement with the nuclear environment [22–27].

To appreciate the non-trivial role of entanglement in the BO picture, consider the exact wave-function of a pure electron-nuclear system in a factorized form [5, 28, 29]

$$\Psi(\mathbf{r},\mathbf{R}) = \phi_{(e)}(\mathbf{r};\mathbf{R})\chi_{(e)}(\mathbf{R}), \tag{1}$$

where

$$\chi_{(e)}(\mathbf{R}) = \left(\int d\mathbf{r}|\Psi(\mathbf{r},\mathbf{R})|^2\right)^{1/2} \tag{2}$$

is the nuclear wave-function ($\int \mathrm{d}\mathbf{R}|\chi_{(e)}(\mathbf{R})|^2 = 1$), and

$$\phi_{(e)}(\mathbf{r};\mathbf{R}) = \Psi(\mathbf{r},\mathbf{R})/\chi_{(e)}(\mathbf{R}) \tag{3}$$

is the conditional probability amplitude of finding electrons at $\mathbf{r}$ given that the nuclear configuration is $\mathbf{R}$ ($\int \mathrm{d}\mathbf{r}|\phi_{(e)}(\mathbf{r};\mathbf{R})|^2 = 1$). This exact decomposition represents an entangled electron-nuclear state because of the dependency of the electronic conditional probability amplitude $\phi_{(e)}(\mathbf{r};\mathbf{R})$ on $\mathbf{R}$. By contrast, in the *crude* Born-Oppenheimer (CBO) approach, the electron-nuclear wave-function is approximated as

$$\Psi(\mathbf{r},\mathbf{R}) \approx \phi(\mathbf{r};\mathbf{R}_0)\tilde{\chi}(\mathbf{R}), \tag{4}$$

where $\phi(\mathbf{r};\mathbf{R}_0)$ is an eigenfunction of the electronic Hamiltonian $H_e(\mathbf{r};\mathbf{R})$ for a particular nuclear configuration $\mathbf{R} = \mathbf{R}_0$, i.e.

$$\hat{H}_e(\mathbf{r};\mathbf{R}_0)\phi(\mathbf{r};\mathbf{R}_0) = E(\mathbf{R}_0)\phi(\mathbf{r};\mathbf{R}_0), \tag{5}$$

and $\tilde{\chi}(\mathbf{R})$ is the nuclear counterpart. Considering that a CBO state is a separable product between a nuclear state and an electronic state [Eq. (4)], the electron-nuclear state is clearly unentangled. The BO states are intermediate between these two limiting situations

$$\Psi(\mathbf{r},\mathbf{R}) \approx \Psi_{\mathrm{BO}}(\mathbf{r},\mathbf{R}) = \phi(\mathbf{r};\mathbf{R})\chi(\mathbf{R}), \tag{6}$$

* artur.izmaylov@utoronto.ca
† ignacio.franco@rochester.edu

where the electronic function $\phi(\mathbf{r};\mathbf{R})$ is obtained as an eigen-function of the electronic Hamiltonian for all nuclear configurations

$$\hat{H}_e(\mathbf{r};\mathbf{R})\phi(\mathbf{r};\mathbf{R}) = E(\mathbf{R})\phi(\mathbf{r};\mathbf{R}). \quad (7)$$

Thus, $\phi(\mathbf{r};\mathbf{R})$ *is* allowed an $\mathbf{R}$ dependence, suggesting that BO states are entangled. However, such a dependency is restricted so that nuclear motion proceeds without changes in the quantum state of the electron cloud, suggesting that the nuclear and electronic dynamics are somewhat less correlated. The main questions are: How entangled are BO states? Does the BO approximation preserves the entanglement character of the exact states? Is there a relation between the degree of entanglement of electron-nuclear states and the validity of the BO approximation?

Here, we address these questions and clarify the role of electron-nuclear entanglement in the BO approximation. This is done through formal considerations and model computations in a two-state one-dimensional system with an avoided crossing. Specifically, we show that BO states are generally entangled except in the limit in which the BO approximation becomes exact. Interestingly, while non-adiabatic couplings can lead to entanglement and to a failure of the BO approximation, entanglement does not necessarily lead to a significant failure of the BO approximation.

The structure of this paper is as follows: Section II introduces purity as a measure of entanglement in the context of electron-nuclear systems. This purity measure is used in Sec. III to analyze the general entangled character of exact and BO states, and the unentangled limit in which the BO approximation becomes formally exact. Section IV introduces a one-dimensional two-state model with an avoided crossing that is used to illustrate numerically the correlation, or lack thereof, between the accuracy of the BO approximation and the degree of entanglement. In Sec. V we summarize our main findings and discuss their implication in the interpretation of coherence phenomena.

II. PURITY AS A MEASURE OF ENTANGLEMENT

As a measure of entanglement between electrons and nuclei we can employ the purity of either the electronic

$$P_e = \mathrm{Tr}\{\hat{\rho}_e^2\}, \quad (8)$$

or nuclear subsystem

$$P_N = \mathrm{Tr}\{\hat{\rho}_N^2\}, \quad (9)$$

where $\hat{\rho}_e = \mathrm{Tr}_N\{\hat{\rho}\}$ ($\hat{\rho}_N = \mathrm{Tr}_e\{\hat{\rho}\}$) is the electronic (nuclear) reduced density matrix obtained by tracing out the nuclear (electronic) degrees of freedom out of the density matrix of the full system $\hat{\rho} = |\Psi\rangle\langle\Psi|$. For unentangled electron-nuclear systems, $P_e = P_N = 1$, while entanglement leads to a non-idempotency of the reduced density matrix and thus P_e and P_N values lower than 1. Such entanglement is a basic source of electronic (or nuclear) decoherence as it leads to a mixed density matrix for the electronic (or nuclear) subsystem.

As a consequence of the Schmidt theorem [11, 30], for pure electron-nuclear systems the electronic and nuclear purity actually coincide, i.e. $P_e = P_N = P$. The Schmidt theorem can be readily verified for the general electron-nuclear state in Eq. (1). The nuclear reduced density matrix is given by

$$\rho_N(\mathbf{R},\mathbf{R}') = \chi_{(e)}(\mathbf{R})\chi^\star_{(e)}(\mathbf{R}')\int \mathrm{d}\mathbf{r}\,\phi_{(e)}(\mathbf{r};\mathbf{R})\phi^\star_{(e)}(\mathbf{r};\mathbf{R}'), \quad (10)$$

where the integral is not a normalization integral since $\mathbf{R}$ and $\mathbf{R}'$ can have different values. The corresponding electronic density matrix is

$$\rho_e(\mathbf{r},\mathbf{r}') = \int \mathrm{d}\mathbf{R}\,|\chi_{(e)}(\mathbf{R})|^2\phi_{(e)}(\mathbf{r};\mathbf{R})\phi^\star_{(e)}(\mathbf{r}';\mathbf{R}). \quad (11)$$

The purity of the electronic and nuclear state coincide since

$$\begin{aligned}\mathrm{Tr}\{\hat{\rho}_e^2\} &= \int \mathrm{d}\mathbf{r}\mathrm{d}\mathbf{r}'\rho_e(\mathbf{r},\mathbf{r}')\rho_e(\mathbf{r}',\mathbf{r}) \\ &= \int \mathrm{d}\mathbf{r}\mathrm{d}\mathbf{r}'\mathrm{d}\mathbf{R}\mathrm{d}\mathbf{R}'|\chi_{(e)}(\mathbf{R})|^2|\chi_{(e)}(\mathbf{R}')|^2\times \\ &\quad \phi^\star_{(e)}(\mathbf{r};\mathbf{R})\phi_{(e)}(\mathbf{r}';\mathbf{R})\phi^\star_{(e)}(\mathbf{r}';\mathbf{R}')\phi_{(e)}(\mathbf{r};\mathbf{R}') \\ &= \int \mathrm{d}\mathbf{R}\mathrm{d}\mathbf{R}'\rho_N(\mathbf{R},\mathbf{R}')\rho_N(\mathbf{R}',\mathbf{R}) \\ &= \mathrm{Tr}\{\hat{\rho}_N^2\} = P.\end{aligned} \quad (12)$$

Naturally, this theorem also applies to BO electron-nuclear states. Therefore, without loss of generality, to quantify entanglement in the exact and BO case we can focus on the purity of the nuclear subsystem. As it turns out, this choice is particularly convenient because of the inherent asymmetry of the BO state.

III. ENTANGLEMENT OF ELECTRON-NUCLEAR STATES

To illustrate the entanglement in terms of purity for the exact [Eq. (1)] and BO [Eq. (6)] electron-nuclear states it is instructive to consider an expansion of their electronic components in the CBO basis $\{\phi_i(\mathbf{r};\mathbf{R}_0)\}$. Since the algebra involved in our consideration is exactly the same for the exact electronic conditional probability and BO electronic state we will derive the purity expression only for the BO case. The electronic BO function can be written as

$$\phi(\mathbf{r};\mathbf{R}) = \sum_i \phi_i(\mathbf{r};\mathbf{R}_0)C_i(\mathbf{R}), \quad (13)$$

which makes the BO electron-nuclear function

$$\begin{aligned}\Psi_{\mathrm{BO}}(\mathbf{r},\mathbf{R}) &= \sum_i \phi_i(\mathbf{r};\mathbf{R}_0)C_i(\mathbf{R})\chi(\mathbf{R}) \\ &= \sum_i \phi_i(\mathbf{r};\mathbf{R}_0)\tilde{\chi}_i(\mathbf{R}).\end{aligned} \quad (14)$$

Here

$$\int \mathrm{d}\mathbf{R}|\tilde{\chi}_i(\mathbf{R})|^2 = \int \mathrm{d}\mathbf{R}|\chi(\mathbf{R})|^2|C_i(\mathbf{R})|^2 \leq 1, \quad (15)$$

which is a consequence of the positivity of the absolute squares and the unit upper boundary for the $|C_i(\mathbf{R})|^2$ function. The equality is only possible for the case when there is only one term in the CBO expansion [Eq. (13)].

Using the CBO basis, the nuclear density expands as

$$\begin{aligned}\rho_N(\mathbf{R},\mathbf{R}') &= \sum_{ij} \tilde{\chi}_i(\mathbf{R})\tilde{\chi}_j^\star(\mathbf{R}')\langle\phi_j(\mathbf{R}_0)|\phi_i(\mathbf{R}_0)\rangle \\ &= \sum_i \tilde{\chi}_i(\mathbf{R})\tilde{\chi}_i^\star(\mathbf{R}'),\end{aligned} \quad (16)$$

where we have taken into account the orthogonality of the CBO states. This form is convenient for illustrating the fact that the nuclear density matrix represents a mixed state due to entanglement:

$$\begin{aligned}P = \mathrm{Tr}\{\hat{\rho}_N^2\} &= \int \mathrm{d}\mathbf{R}\mathrm{d}\mathbf{R}'\rho_N(\mathbf{R},\mathbf{R}')\rho_N(\mathbf{R}',\mathbf{R}) \\ &= \sum_{ij}\langle\tilde{\chi}_j|\tilde{\chi}_i\rangle\langle\tilde{\chi}_i|\tilde{\chi}_j\rangle.\end{aligned} \quad (17)$$

Substituting $S_{ij} = \langle\tilde{\chi}_i|\tilde{\chi}_j\rangle$ we have

$$P = \sum_{ij}|S_{ij}|^2 \leq \sum_{ij} S_{ii}S_{jj} = 1, \quad (18)$$

where we have taken into account the Schwarz inequality and the normalization condition $\sum_i S_{ii} = 1$. The equality in Eq. (18) is only possible for two special cases: when there is only a single term in the CBO expansion or when all nuclear components $\tilde{\chi}_i$ are equal to each other up to constant multiplicative factors. Thus, Eq. (18) clearly shows that for general electron-nuclear states, exact or BO, are generally entangled, as expected.

A complementary perspective on the origin of entanglement in electron-nuclear states can be gleaned from the purity of the BO state without performing the CBO expansion

$$P = \int \mathrm{d}\mathbf{R}\mathrm{d}\mathbf{R}'|\chi(\mathbf{R})|^2|\chi(\mathbf{R}')|^2|\langle\phi(\mathbf{R})|\phi(\mathbf{R}')\rangle|^2. \quad (19)$$

The electronic part $|\langle\phi(\mathbf{R})|\phi(\mathbf{R}')\rangle|^2$ can be bound from above by the Schwartz inequality

$$|\langle\phi(\mathbf{R})|\phi(\mathbf{R}')\rangle|^2 \leq \langle\phi(\mathbf{R})|\phi(\mathbf{R})\rangle\langle\phi(\mathbf{R}')|\phi(\mathbf{R}')\rangle = 1 \quad (20)$$

As in Eq. (18), for general electronic wavefunctions the equality in Eq. (20) is not relevant as any nuclear dependence in $|\langle\phi(\mathbf{R})|\phi(\mathbf{R}')\rangle|^2$ leads to values lower than 1. Taking into account the normalization of $\chi(\mathbf{R})$ and that $|\chi(\mathbf{R})|^2 > 1$, it follows that any nuclear dependence in $|\langle\phi(\mathbf{R})|\phi(\mathbf{R}')\rangle|^2$ also results in $P < 1$. Naturally, this result is consistent with the CBO expansion because a nuclear dependence of the electronic wave-function leads to multiple terms in the CBO expansion. To elucidate this dependence let us consider the expansion of the BO electronic wavefunction $\phi(\mathbf{r};\mathbf{R}') = \phi(\mathbf{r};\mathbf{R}+\mathbf{a})$ in Eq. (10) around $\mathbf{R}' = \mathbf{R}$ ($\mathbf{a} = 0$):

$$\begin{aligned}\phi(\mathbf{r};\mathbf{R}+\mathbf{a}) &= \exp\left(\frac{i}{\hbar}\mathbf{a}\cdot\hat{\mathbf{P}}\right)\phi(\mathbf{r};\mathbf{R}) \\ &= \sum_{n=0}^{\infty}\frac{1}{n!}\left(\frac{i}{\hbar}\mathbf{a}\cdot\hat{\mathbf{P}}\right)^n\phi(\mathbf{r};\mathbf{R}),\end{aligned} \quad (21)$$

where $\hat{\mathbf{P}} = -i\hbar\partial_{\mathbf{R}}$ is the total nuclear momentum operator. Inserting Eq. (21) into Eq. (10) yields

$$\begin{aligned}\rho_N(\mathbf{R},\mathbf{R}+\mathbf{a}) = \chi(\mathbf{R})\chi^\star(\mathbf{R}+\mathbf{a})(1+ \\ \sum_{n=1}^{\infty}\frac{1}{n!}\langle\phi(\mathbf{R})|\left(\frac{i}{\hbar}\mathbf{a}\cdot\hat{\mathbf{P}}\right)^n|\phi(\mathbf{R})\rangle).\end{aligned} \quad (22)$$

The first term corresponds to the pure (idempotent) nuclear density matrix. Any entanglement is introduced by the second term governed by the derivatives of the electronic wave-functions with respect to the nuclear coordinates. The BO approximation assumes a weak dependence of the electronic wave-functions on the nuclear configuration. In the limit where the BO approximation is *exact* all derivatives in Eq. (22) should be zero. In this limit, the electron-nuclear states become unentangled, and the expansion of the electron-nuclear state in the CBO basis consists of only one term [cf. Eq. (13)]. However, note that even a mild dependence of the electronic states on the nuclear coordinates can lead to appreciable entanglement. This effect is particularly important when the nuclear state is highly delocalized in space such that the terms $\chi(\mathbf{R})\chi^\star(\mathbf{R}+\mathbf{a})\langle\phi(\mathbf{R})|\left(\frac{i}{\hbar}\mathbf{a}\cdot\hat{\mathbf{P}}\right)^n|\phi(\mathbf{R})\rangle$ are appreciable even for large n's. The delocalization of the nuclear wave-function makes both $\chi(\mathbf{R})$ and $\chi(\mathbf{R}+\mathbf{a})$ appreciable even for large $||\mathbf{a}||$. In turn, a large $||\mathbf{a}||$ enhances the whole term due to its n^{th} power even for small derivatives of the electronic wave-function. For this reason, as discussed in Sec. IV B, for nuclear states with a strong degree of spatial delocalization the adequacy of the BO approximation is not necessarily correlated with the degree of entanglement of the states.

IV. ENTANGLEMENT IN AN AVOIDED CROSSING MODEL

We exemplify the relation between entanglement and the validity of the BO approximation on a minimal model for an avoided crossing (AC) problem (or one-dimensional spin-boson model) [31]. The AC model is one of the simplest cases where breakdown of the BO approximation can be modeled easily [32, 33].

A. Theory and Model

a. Model Hamiltonian: We introduce two diabatic states, $|\varphi_1\rangle$ and $|\varphi_2\rangle$, which will represent the complete

set of CBO basis functions $\{\phi_i(\mathbf{r};\mathbf{R}_0)\}$ [34], and whose explicit electronic coordinate dependence will not be of importance. Presenting the total wave-function as

$$|\Psi\rangle = |\tilde{\chi}_1\rangle|\varphi_1\rangle + |\tilde{\chi}_2\rangle|\varphi_2\rangle, \tag{23}$$

we project the total time-independent Schrödinger equation (TISE) onto the electronic states $\{|\varphi_i\rangle\}_{i=1,2}$

$$\hat{H}\begin{pmatrix}|\tilde{\chi}_1\rangle\\|\tilde{\chi}_2\rangle\end{pmatrix} = E\begin{pmatrix}|\tilde{\chi}_1\rangle\\|\tilde{\chi}_2\rangle\end{pmatrix}, \tag{24}$$

where

$$\hat{H} = \hat{T}\mathbf{1}_2 + \begin{pmatrix}V_{11} & V_{12}\\ V_{12} & V_{22}\end{pmatrix}, \tag{25}$$

$\hat{T} = -\frac{1}{2}\partial_x^2$ is the nuclear kinetic energy operator (the units are chosen such that $\hbar = m = 1$ and, for simplicity, the nuclear subspace contains only one coordinate $\mathbf{R} = x$), and $\mathbf{1}_2$ is a 2×2 unit matrix. The diabatic potentials V_{11} and V_{22} are identical 1D parabolas shifted in the x-direction by a and in energy by Δ, i.e.

$$V_{11} = \frac{\omega^2 x^2}{2}, \tag{26}$$

$$V_{22} = \frac{\omega^2}{2}(x-a)^2 + \Delta. \tag{27}$$

To have an avoided crossing in the adiabatic representation V_{11} and V_{22} are coupled by a constant potential $V_{12} = c$.

Switching to the adiabatic representation for the 1D AC Hamiltonian in Eq. (25) is done by diagonalizing the potential matrix using a unitary transformation

$$U = \begin{pmatrix}\cos\theta & \sin\theta\\ -\sin\theta & \cos\theta\end{pmatrix}, \tag{28}$$

where $\theta = \theta(x)$ is a mixing angle in the superposition between the diabatic electronic states states $|\varphi_1\rangle$ and $|\varphi_2\rangle$, and is given by

$$\theta = \frac{1}{2}\arctan\frac{2\,V_{12}}{V_{11}-V_{22}} = \frac{1}{2}\arctan\frac{\gamma}{x-b}. \tag{29}$$

Here, $b = \Delta/(\omega^2 a)$ is the x-coordinate of the crossing point, and

$$\gamma = 2c/(\omega^2 a) \tag{30}$$

is a coupling strength between the diabatic states.

The transformation $U(\theta)$ defines the BO electronic states

$$|\phi_1(x)\rangle = \quad \cos\theta\,|\varphi_1\rangle + \sin\theta\,|\varphi_2\rangle \tag{31}$$

$$|\phi_2(x)\rangle = -\sin\theta\,|\varphi_1\rangle + \cos\theta\,|\varphi_2\rangle \tag{32}$$

and gives rise to the 1D AC Hamiltonian in the adiabatic representation $\hat{H}_{\rm adi} = U\hat{H}U^\dagger$,

$$\hat{H}_{\rm adi} = \begin{pmatrix}\hat{T}+\hat{\tau}_{11} & \hat{\tau}_{12}\\ \hat{\tau}_{21} & \hat{T}+\hat{\tau}_{22}\end{pmatrix} + \begin{pmatrix}W_- & 0\\ 0 & W_+\end{pmatrix}, \tag{33}$$

where

$$W_\pm = \frac{1}{2}\left(V_{11}+V_{22}\right) \pm \frac{1}{2}\sqrt{\left(V_{11}-V_{22}\right)^2 + 4V_{12}^2} \tag{34}$$

are the adiabatic potentials and $\hat{\tau}_{ij} = -\langle\phi_i(x)|\partial_x\phi_j(x)\rangle\,\partial_x - \frac{1}{2}\langle\phi_i(x)|\partial_x^2\phi_j(x)\rangle$ are the nonadiabatic couplings (NACs). For this model, the NACs can be expressed as

$$\hat{\tau}_{11} = \hat{\tau}_{22} = \frac{1}{2}[\partial_x\theta(x)]^2, \tag{35}$$

$$\hat{\tau}_{21} = -\hat{\tau}_{12} = -\partial_x\theta(x)\partial_x - \frac{1}{2}\partial_x^2\theta(x). \tag{36}$$

The BO approximation neglects all nonadiabatic terms $\hat{\tau}_{ij}$ and formulates the nuclear TISE as

$$[\hat{T} + W_\pm(x)]\chi(x) = E_{BO}\chi(x). \tag{37}$$

The adequacy of the BO approximation in this model depends on the NAC element

$$\begin{aligned}\langle\phi_2(x)|\partial_x\phi_1(x)\rangle =& \partial_x\theta(x)\\ =& \frac{\gamma}{4\gamma^2+(x-b)^2}.\end{aligned} \tag{38}$$

The maximum of $\partial_x\theta(x)$ is at the crossing point $x = b$ and has a simple dependence on model parameters

$$(\partial_x\theta)_{\max} = \frac{1}{4\gamma}. \tag{39}$$

Although it may seem that Eq. (39) provides a straightforward way to predict the failure or success of the BO approximation, to get an accurate assessment one also needs to consider the nuclear density at the vicinity of the crossing point b. This is because $\langle\phi_2(x)|\partial_x\phi_1(x)\rangle$ is part of the nuclear kinetic energy operator in Eq. (33) and, therefore, without non-negligible nuclear density a large NAC value will not have a significant effect.

b. Purity: As for entanglement measured in terms of the purity, Eq. (18) for this two-state case can be expressed as

$$\begin{aligned}{\rm Tr}[\hat{\rho}_N^2] =& (S_{11}+S_{22})^2 - 2(S_{11}S_{22} - S_{12}^2)\\ =& 1 - 2(S_{11}S_{22} - S_{12}^2).\end{aligned} \tag{40}$$

This shows that the loss of purity comes from the interplay between diagonal and off-diagonal nuclear overlap matrix elements S_{ij}. For exact and BO states, we will refer to nuclear states with $S_{ii} \gg S_{jj}$ as *localized* and those with $S_{11} \approx S_{22} \approx 1/2$ as *delocalized*. Note that due to the Schwarz inequality $S_{11}S_{22} \geq S_{12}^2$ and the normalization condition $S_{11}+S_{22} = 1$, the localization condition $S_{ii} \gg S_{jj}$ always leads to vanishing S_{12}^2, whereas the delocalization condition $S_{11} \approx S_{22} \approx 1/2$ does not require S_{12} to be small.

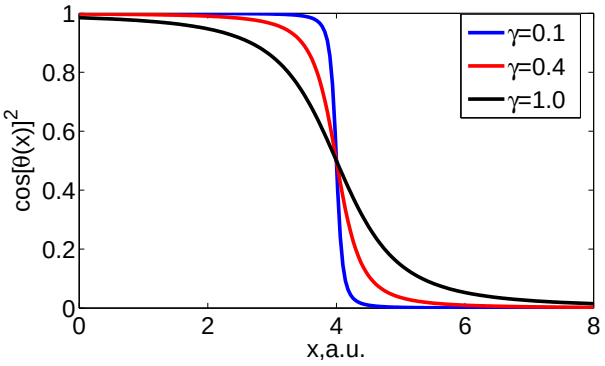


FIG. 1. The partitioning function $\cos[\theta(x)]^2$ for different γ's and the crossing point for two parabolas $b = 4$ a.u.

c. BO wave-function: To analyze entanglement in the BO wave-function, without loss of generality [35] we focus on the ground electronic state wave-function expressed in the diabatic basis

$$\begin{aligned}\langle x|\Psi_{BO}\rangle =&\langle x|\chi\rangle|\phi_1(x)\rangle\\ =&\langle x|\chi\rangle(C_1(x)|\varphi_1\rangle + C_2(x)|\varphi_2\rangle)\\ =&\langle x|\tilde{\chi}_1\rangle|\varphi_1\rangle + \langle x|\tilde{\chi}_2\rangle|\varphi_2\rangle,\end{aligned} \tag{41}$$

where $\langle x|\tilde{\chi}_1\rangle = \chi(x)\cos[\theta(x)]$ and $\langle x|\tilde{\chi}_2\rangle = \chi(x)\sin[\theta(x)]$ are the nuclear components in the diabatic basis. The terms $\cos[\theta(x)]^2$ and $\sin[\theta(x)]^2$, depicted in Fig. 1, can be thought as partitioning functions that split the nuclear BO probability density $|\chi|^2$ into the diabatic components $|\tilde{\chi}_1|^2$ and $|\tilde{\chi}_2|^2$. As exemplified in Fig. 1, these complementary partitioning functions go from 0 to 1 around $x = b$ in a characteristic length proportional to γ. This γ-dependence arises because $\partial_x \cos[\theta(x)]^2 \sim \partial_x \sin[\theta(x)]^2 \sim \partial_x\theta(x)$ and Eq. (38).

Using these partitioning functions, the S_{12}^2 part of Eq. (40) can be expressed as

$$\begin{aligned}S_{12}^2 =&\left(\int dx\chi^2(x)\cos[\theta(x)]\sin[\theta(x)]\right)^2\\ =&\frac{1}{4}\left(\int dx\chi^2(x)\sin\left[\arctan\left(\frac{\gamma}{x-b}\right)\right]\right)^2\\ =&\frac{1}{4}\left(\int dx\frac{\chi^2(x)}{\sqrt{\gamma^2+(x-b)^2}}\right)^2.\end{aligned} \tag{42}$$

Therefore, S_{12} will be large if the BO nuclear probability density $\chi^2(x)$ is high at the intersection point $x = b$. Also, S_{12}^2 can be bound from above using the Schwarz inequality

$$\begin{aligned}S_{12}^2 \leq&\frac{1}{4}\int dx\chi^4(x)\int\frac{dx}{\gamma^2+(x-b)^2}\\ =&\gamma\frac{\pi}{4}\int dx\chi^4(x).\end{aligned} \tag{43}$$

Hence, $S_{12}^2 \sim \gamma$, which allows us to simplify the purity in the limiting case of divergent NACs (recall Eq. (39))

$$\lim_{\gamma\to 0} P_N = 1 - 2S_{11}S_{22} \approx \begin{cases} 1, \text{ if } S_{ii} \gg S_{jj} \\ 1/2, \text{ if } S_{ii} \approx 1/2. \end{cases} \tag{44}$$

In turn, when γ is appreciable, S_{12}^2 can become comparable with $S_{11}S_{22}$ and this leads to an increased purity up to $P_N \approx 1$. In the limit of $\gamma \to \infty$ the BO approximation is exact and the purity goes to 1. One of the simplest ways to see this is to consider the $a \to 0$ approach to the $\gamma \to \infty$ limit. If $a \to 0$, the two parabolas will always be parallel to each other and a unitary transformation diagonalizing the potential matrix [Eq. (25)] in one nuclear configuration will diagonalize it for all other configurations. Therefore the CBO and BO states will be identical which is enough for the purity to be 1 [see Eq. (18)]. Other approaches to the $\gamma \to \infty$ limit ($\omega \to 0$ and $c \to \infty$) give the same result. Also, in the $\gamma \to \infty$ limit the exact and BO states coincide because nonadiabatic couplings are zero. Therefore we will not focus on large γ's in the numerical examples presented below.

B. Numerical Examples

To quantitatively investigate the correlation between the adequacy of the BO approximation and the degree of entanglement, we consider three model cases defined by the parameters in Table I. The PES associated with each of the models are shown in Figs. 2a-4a. In each case, entanglement is quantified through the purity, while the adequacy of the BO approximation is assessed by examining the difference of the exact total energy E [Eq. (24)] with that obtained in the BO approximation E_{BO}, as well as the magnitude of the overlap between the corresponding electron-nuclear wave-functions $|\langle\Psi|\Psi_{BO}\rangle|$.

1. *Entanglement in stationary states*

TABLE I. Parameters of the three model two-level systems with Hamiltonian Eq. (25). In all models, $\omega = 1$ and $c = \omega/5$ a.u.

Model	a	Δ	γ
1	4	0	0.1
2	4	1.5 ω	0.1
3	1	4 ω	0.4

a. Model 1: Corresponds to a case in which the ground PES has two degenerate minima, while the excited PES has a single minimum located at the midpoint between the ground-state minima, see Fig. 2a. The first few states in this model are well described by the BO approximation (Fig. 2b and c) because their nuclear

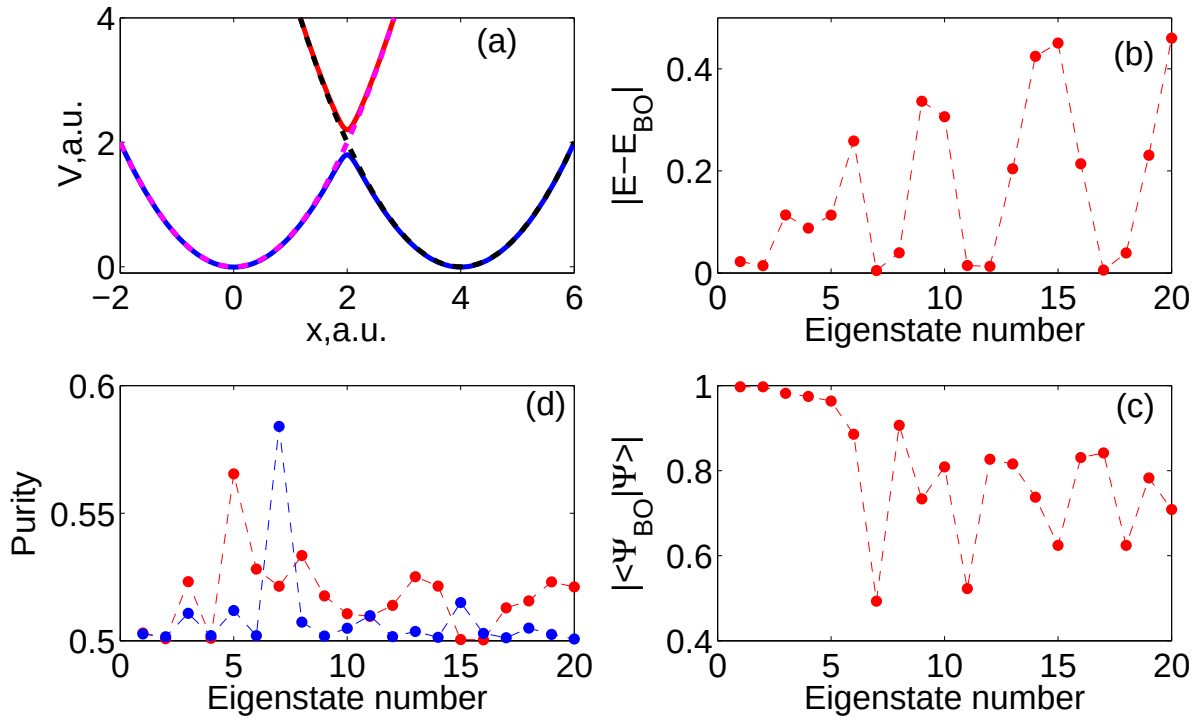


FIG. 2. Model 1: (a) Adiabats (solid) and diabats (dashed); (b) Absolute energy differences between exact and BO eigen-states; (c) Absolute overlaps between exact and BO eigen-functions; (d) Purities of the BO (blue) and exact (red) eigen-states.

wave-functions do not have large probability density in the vicinity of the NAC function maximum [Eq. (39)]. The first state that has a substantial deviation from the exact wave-function according to the overlap criterion is the 7^{th} BO state. The reason for the large discrepancy is that the 7^{th} BO state is the ground vibrational state on the excited electronic BO-PES. Thus, it has large nuclear probability density in the vicinity of the NAC maximum. Higher energy states in the BO approximation correspond to either the excited or the ground electronic states. Generally, the overlap with the exact wave-function is better for the BO states of the ground electronic state. Since the ordering of the eigen-states is done based on their energies, alternation of states from the ground and excited BO-PES creates oscillations in absolute overlaps in Fig. 2c.

For most states considered, the purity is close to 1/2 both in the exact and BO treatments (Fig. 2d). That is, the BO states approximately preserve the entangled character of the exact states. This takes place for both methods because nuclear overlaps S_{12} are small and the nuclear component of the eigenstates is delocalized ($S_{11} \approx S_{22} \approx 1/2$). To understand the delocalization in the exact wave-functions one can use first order perturbation theory to estimate the relative contributions of the diabatic vibrational states to the nuclear component of the exact wave-function: The low coupling (c) between the diabatic vibrational states is overpowered by the vibrational level alignment of two parabolas (as $\Delta = 0$). Degenerate perturbation theory yields equal contributions of the two diabatic degenerate states to the eigenstates. In this case, the S_{12} elements are Franck-Condon overlaps between energetically aligned diabatic vibrational states and they are small as a result of a relatively large spatial shift $a = 4$. In turn, the BO states are generally delocalized due to the symmetry of BO-PESs $W_{\pm}$. The low magnitude for the overlaps S_{12} is a result of a small γ [Eq. (43)]. The only appreciable increase in purity across the BO states can be seen for the 7^{th} state, because of the highest localization of nuclear probability density at the crossing region in this state and as a result an increased overlap S_{12} [see Eqs. (42) and (40)].

In this model, the BO eigenstates provide a clear example of a system in which the BO approximation is appropriate (albeit not exact) but where the (exact and BO) electron-nuclear states are maximally entangled.

b. Model 2: By introducing an electronic energy shift $\Delta = 1.5\omega$ which breaks the diabatic vibrational level alignment of Model 1, the exact wave-functions now acquire a high degree of localization. In perturbation theory terms, a relatively small coupling $c = \omega/5$ cannot generate appreciable contributions from the vibrational states of the two diabats when the minimal energy difference between levels is $\omega/2$. In turn, in the BO approximation this localization is present only in the first few states which are localized in the lower energy well. De-

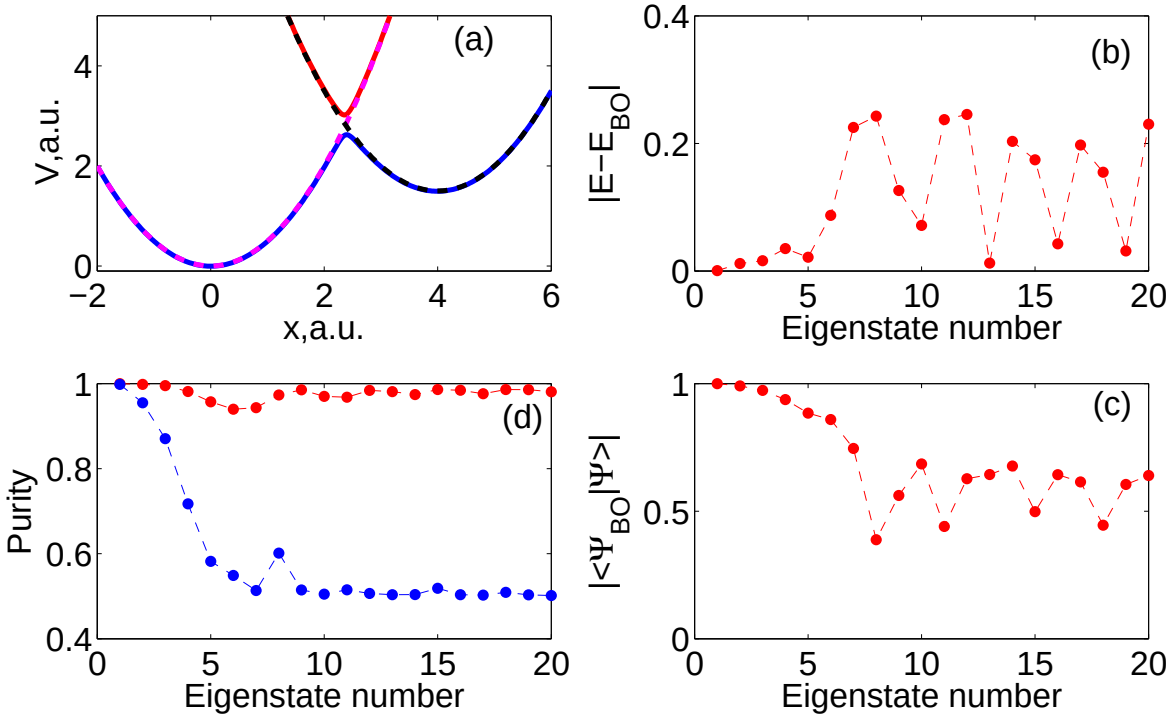


FIG. 3. Model 2: (a) Adiabats (solid) and diabats (dashed); (b) Absolute energy differences between exact and BO eigen-states; (c) Absolute overlaps between exact and BO eigen-functions; (d) Purities of the BO (blue) and exact (red) eigen-states.

localization of the higher energy states in BO leads to a failure of the BO approximation for these states (Figs. 3b and c). The localization in the exact wave-functions leads to $S_{12} \approx 0$ and $S_{11}S_{22} \approx 0$ in Eq. (40), and therefore, the purity for all states is very close to 1 (Fig. 3d). In contrast, the purity in the BO approximation quickly drops to 1/2 because of the states' delocalization [Eq. (44)].

This model exemplifies a case in which the exact eigenstates are approximately unentangled, while the corresponding BO states can be strongly entangled. For some of these states (i.e. state 5) the disparity between the degree of entanglement between the exact and BO states leads to only modest energetic errors. That is, the BO state can be adequate from an energetic perspective even when the entanglement content of the BO state is a poor approximation to the exact eigenstate.

c. Model 3: Owing to the electronic energy shift $\Delta = 4\omega$ that preserves an energetic alignment of the diabatic vibrational levels, and a smaller coordinate shift, $a = 1$, the high energy exact wave-functions of this model consist of almost equal contributions from the two diabatic states. Nuclear functions $\tilde{\chi}_1$ and $\tilde{\chi}_2$ corresponding to these contributions are almost orthogonal ($S_{12} \approx 0$ in Eq. (40)) due to a very different number of nodes in energetically aligned vibrational states from the two parabolas. This leads to the purity close to 1/2 for these states (Fig. 4d).

As in Model 2, the BO approximation is adequate only for lower states where both methods produce localized nuclear wave-functions (Figs. 4b and c). In this case, the purity and energy of the BO states is an excellent approximation to the exact states. Naturally, the purity for these low states is close to 1 (Fig. 4d). However, in contrast to Model 2, the purity of BO states stays close to 1 even for higher excited states because of persistent localization of states that makes the product $S_{11}S_{22}$ and overlaps S_{12} in Eq. (40) small. In spite of the higher value of γ in this model wth respect to the other models, localized states occur here because of a disproportional partitioning of the nuclear BO wave-function into large and small (norm-wise) diabatic components $\tilde{\chi}_1$ and $\tilde{\chi}_2$. This disproportionality originates from the right shift of the diabatic intersection point, $b = 4$ (Fig. 4a), which regulates the partitioning location (see Fig. 1). Such a right shifted partitioning of the BO nuclear probability density produces one nuclear component which is dominant and the other one that only represents a small tail of the original distribution. Thus, in Model 3, we have states where the BO approximation breaks down even when the BO eigenstates are only weakly entangled.

2. *Entanglement in non-stationary states*

To illustrate the behavior of the purity for non-stationary BO states we now consider two cases where

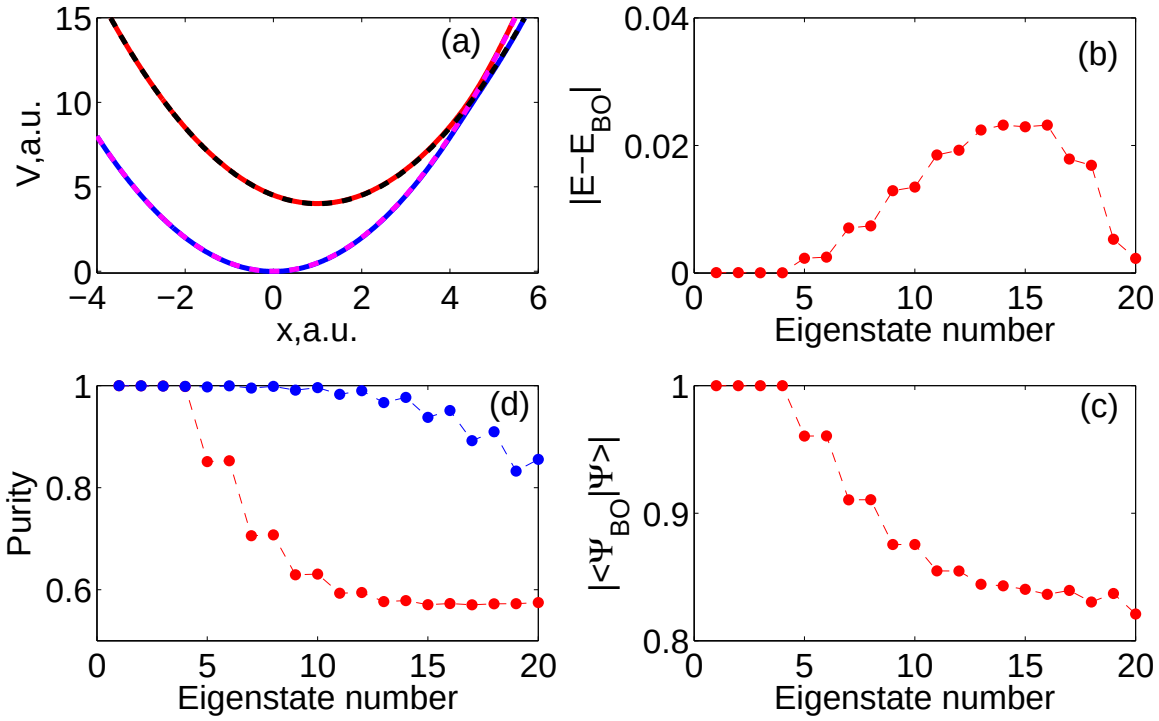


FIG. 4. Model 3: (a) Adiabats (solid) and diabats (dashed); (b) Absolute energy differences between exact and BO eigen-states; (c) Absolute overlaps between exact and BO eigen-functions; (d) Purities of the BO (blue) and exact (red) eigen-states.

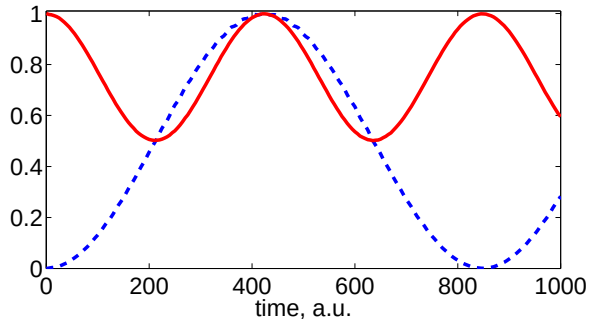


FIG. 5. The average nuclear position (dashed blue) and purity P_N (solid red) as functions of time for Model 1 BO dynamics with a non-stationary nuclear wave-packet.

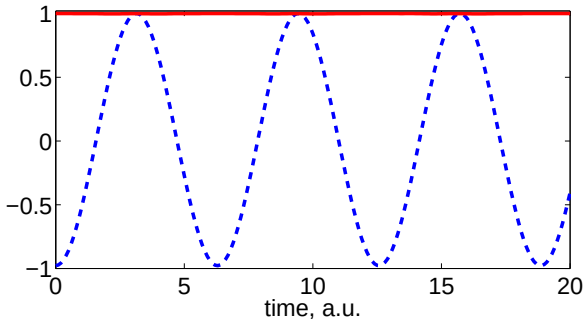


FIG. 6. The average nuclear position (dashed blue) and purity P_N (solid red) as functions of time for Model 3 BO dynamics with a non-stationary nuclear wave-packet.

the dynamics is adequately represented by the BO approximation. First, in Model 1, an initial wave-packet has been taken as a ground state of the diabatic uncoupled parabola

$$\chi(x) = \left(\frac{\omega}{\pi}\right)^{1/4} \exp\left(-\frac{\omega(x-x_0)^2}{2}\right), \qquad (45)$$

it has been centred at the bottom of the left well $x_0 = 0$. In the BO representation, this wave-packet is mostly comprised of the two lowest energy eigen-states of the double well problem; symmetric and anti-symmetric wave-functions which after summation give localization in a single well. Due to the superposition nature, this initial nuclear wave-packet will tunnel back and forth between two wells. Figure 5 presents both coherent oscillations of the left well population and the purity dynamics. Naturally, the purity is 1 at the end points corresponding to localization of a wave-packet within a particular well, while it drops as low as 1/2 during the period of coherent oscillations.

Second, in Model 3, the same initial wave-packet [Eq. (45)] has been placed on the left slope ($x_0 = -1$

a.u.) of the lower potential. This wave-packet represents a coherent superposition of low energy BO vibrational states which do not have enough energy to transfer on to the upper BO electronic state. Thus, wave-packet dynamics represents vibrational coherent oscillations at the bottom of the lowest BO state without changing the purity of the wave-packet over time (Fig. 6).

3. *Criterion for disentanglement of BO states*

For devising a simple qualitative picture to understand entanglement for an arbitrary electron-nuclear state, it is useful to introduce the notion of nuclear function support. We define a function support as a collection of x-ranges where the function has non-negligible value. Then we introduce a domain of adequacy for each CBO configuration as an x-range where the BO electronic wave function has a dominant contribution from this CBO configuration (e.g., $|C_i(\mathbf{R})| \gg |C_j(\mathbf{R})|$ for $\forall j \neq i$). There are also intermediate regions in the x-space where the BO electronic function can have comparable contributions from different CBO configurations. If the nuclear component has a functional support in these regions the BO approximation can become inadequate, and therefore, entanglement considerations would require accounting for nonadiabatic effects. In cases where the BO approximation is adequate and the nuclear function support is located only in domains of adequacy for single CBO configurations, a simple estimate can be made for the BO state purity. If the support of the nuclear function $\chi(x)$ spans N_D single CBO configuration domains, $\mathcal{D}_i$, then the purity will be

$$P_N \approx \sum_{i=1}^{N_D} \omega_i^2, \tag{46}$$

where individual domain weights are given by

$$\omega_i = \int_{\mathcal{D}_i} |\chi(x)|^2 dx. \tag{47}$$

Thus, if we extend our model to N 1D parabolic potentials all shifted along the x-axis consequentially from the origin and constantly coupled, then the purity of the ground state will be $1/N$. This setup can be thought as a finite model for a periodic system, and it shows that entanglement of the ground BO state can be made indefinitely strong by increasing N.

V. FINAL REMARKS

The formal and numerical results presented above show that when the BO approximation is exact ($\gamma \to \infty$ for the AC model) the resulting BO states are unentangled. However, in the usual situation in which the BO strategy is an approximation the resulting BO states will generally be entangled. Contrary to intuition, we find that while non-adiabatic couplings can lead to electron-nuclear entanglement and to a failure of the BO approximation, the degree of entanglement of a BO state and the degree of validity of the BO approximation are generally uncorrelated. Thus, it is possible to find accurate BO states with a high degree of entanglement and poor BO states with a low entanglement level. Further, the purity of the BO states can either be higher or lower than that of the exact eigenstates.

The reason for this counterintuitive behavior is that while the degree of entanglement of BO states is determined by their deviation from the corresponding states in the crude BO approximation, the accuracy of the BO approximation is dictated, instead, by the deviation of the BO states from the exact electron-nuclear states. These two metrics are not necessarily simply connected and this explains the absence of an apparent correlation.

The intuitive picture is restored in the limit where the BO states coincide with the CBO states (c.f. the first few levels in Model 3). In this limit, any entanglement in the BO state also signals a decay in the validity of the BO approximation. By contrast, when the BO states are very different from the corresponding CBO states, this intuition does not hold any more. This was dramatically illustrated by the double-well problem in Model 1, that involve "nonlocal" BO states with nuclear probability amplitude associated with distinct electronic *diabatic* states. These states are seen to be strongly entangled even when the BO states provide a useful approximation to the exact states.

In fact, we find that a more adequate criterion for unentanglement of BO states is to require that the nuclear wave-function support is within the domain of adequacy of a single CBO configuration. Entanglement in the BO state is inevitable if this support spans a region where more than one CBO configuration contributes to the BO state. The implication is that in molecules, electron-nuclear entanglement and thus electronic decoherence can occur even in the ground-state, zero-temperature, BO approximation.

Importantly, we observe that the BO approximation does not necessarily preserve the entanglement character of the exact states even when the BO approximation is adequate from an energetic perspective. This fact complicates the interpretation of coherence phenomena for electrons in molecules. This is because the degree of coherence for the electronic subsystem when the electron-nuclear system is in a given superposition of exact eigenstates can be very different from that predicted by the same superposition but among the BO equivalents to the exact eigenstates. This implies that analyzing electronic coherences starting from BO states for the system plus bath should involve consideration of how accurately those states preserve the entanglement properties of the exact states.

VI. ACKNOWLEDGEMENTS

A.F.I. thanks R. Kapral, I. G. Ryabinkin, and P. Brumer for helpful discussions and acknowledges funding from the Natural Sciences and Engineering Research Council of Canada (NSERC) through the Discovery Grants Program and the Alfred P. Sloan Foundation. I.F. acknowledges support by the National Science Foundation under CHE - 1553939.

[1] R. Kapral and G. Ciccotti, J. Chem. Phys. **110**, 8919 (1999).
[2] J. C. Tully, J. Chem. Phys. **93**, 1061 (1990).
[3] M. Ben-Nun and T. J. Martinez, Advances in chemical physics **121**, 439 (2002).
[4] P. Huo and D. F. Coker, J. Chem. Phys. **135**, 201101 (2011).
[5] A. Abedi, N. T. Maitra, and E. K. U. Gross, Phys. Rev. Lett. **105**, 123002 (2010).
[6] A. F. Izmaylov, D. Mendive Tapia, M. J. Bearpark, M. A. Robb, J. C. Tully, and M. J. Frisch, J. Chem. Phys. **135**, 234106 (2011).
[7] A. F. Izmaylov, J. Chem. Phys. **138**, 104115 (2013).
[8] J. S. Endicott, L. Joubert-Doriol, and A. F. Izmaylov, J. Chem. Phys. **141**, 034104 (2014).
[9] E. Schrödinger, Naturwissenschaften **23**, 807 (1935).
[10] A. Einstein, B. Podolsky, and N. Rosen, Phys. Rev. **47**, 777 (1935).
[11] M. A. Nielsen and I. L. Chuang, *Quantum Computation and Quantum Information*, 10th ed. (Cambridge University Press, New York, NY, USA, 2011).
[12] J. C. Tully, J. Chem. Phys. **137**, 22A301 (2012).
[13] J. E. Subotnik, A. Jain, B. Landry, A. Petit, W. Ouyang, and N. Bellonzi, Ann. Rev. Phys. Chem. **67** (2016).
[14] B. G. Levine and T. J. Martínez, Annu. Rev. Phys. Chem. **58**, 613 (2007).
[15] Y.-C. Cheng and G. R. Fleming, Annu. Rev. Phys. Chem. **60**, 241 (2009).
[16] G. S. Engel, T. R. Calhoun, E. L. Read, T.-K. Ahn, T. Mančal, Y.-C. Cheng, R. E. Blankenship, and G. R. Fleming, Nature **446**, 782 (2007).
[17] E. Collini, C. Y. Wong, K. E. Wilk, P. M. G. Curmi, P. Brumer, and G. D. Scholes, Nature **463**, 644 (2010).
[18] A. Ishizaki and G. R. Fleming, Annu. Rev. Condens. Matter Phys. **3**, 333 (2012).
[19] L. A. Pachón and P. Brumer, Phys. Chem. Chem. Phys. **14**, 10094 (2012).
[20] F. Ortmann, F. Bechstedt, and K. Hannewald, Phys. Rev. B **79**, 235206 (2009).
[21] S. H. Choi, C. Risko, M. C. R. Delgado, B. Kim, J.-L. Brédas, and C. D. Frisbie, J. Am. Chem. Soc. **132**, 4358 (2010).
[22] M. Schlosshauer, *Decoherence and the Quantum-to-Classical Transition* (Springer, New York, 2008).
[23] E. Joos, H. D. Zeh, C. Kiefer, D. J. W. Giulini, J. Kupsch, and I. O. Stamatescu, *Decoherence and the Appearance of a Classical World in Quantum Theory*, 2nd ed. (Springer, 2003).
[24] A. Kar, L. Chen, and I. Franco, J. Phys. Chem. Lett. **7**, 1616 (2016).
[25] I. Franco and H. Appel, J. Chem. Phys. **139**, 094109 (2013).
[26] I. Franco, A. Rubio, and P. Brumer, New J. Phys. **15**, 043004 (2013).
[27] I. Franco and P. Brumer, J. Chem. Phys. **136**, 144501 (2012).
[28] G. Hunter, Int. J. Quantum Chem.. **9**, 237 (1975).
[29] A. Abedi, N. T. Maitra, and E. K. U. Gross, J. Chem. Phys. **137** (2012).
[30] E. Schmidt, Math. Annalen **63**, 433 (1907).
[31] A. Nitzan, *Chemical Dynamics in Condensed Phases: Relaxation, Transfer, and Reactions in Condenced Molecular Systems* (Oxford University Press, New York, 2006).
[32] B. R. Landry and J. E. Subotnik, J. Chem. Phys. **135**, 191101 (2011).
[33] R. Gherib, L. Ye, I. G. Ryabinkin, and A. F. Izmaylov, J. Chem. Phys. **144**, 154103 (2016).
[34] This equivalence is true up to a constant unitary transformation diagonalizing a matrix of the electronic Hamiltonian within the two-state subspace at the $\mathbf{R_0}$ configuration.
[35] All subsequent derivations for the S_{12} quantity can be repeated with the excited electronic state arriving at the same outcome.